Reprinted from

MECHANICS OF MATERIALS

AN INTERNATIONAL JOURNAL

Mechanics of Materials 22 (1996) 51-64

Number of grains required to homogenize elastic properties of polycrystalline ice

Alex A. Elvin

Massachusetts Institute of Technology, Department of Civil and Environmental Engineering, Room 5-330A, Cambridge, MA 02139, USA

Received 15 March 1995; revised version received 21 August 1995

ELSEVIER

196 B

MECHANICS OF MATERIALS

Aims and Scope

Mechanics of Materials provides a forum for original scientific research on the flow, fracture, and general constitutive behavior of geophysical, geotechnical and technological materials, with balanced coverage of theoretical, experimental, and field investigations. Of special concern are macroscopic predictions based on microscopic models, identification of microscopic structures from limited overall macroscopic date, experimental and field results that lead to fundamental understanding of the behavior of materials, and coordinated experimental and analytical investigations that culminate in theories with predictive quality. The Journal publishes original contributions on the thermomechanical behavior of technological materials such as metals, polymers, ceramics, wood, and others, geotechnical materials such as rock ans soil, and on all thermomechanical processes pertaining to solid earth geophysics.

Abstracted/indexed in:

Applied Mechanics Review; Current Contents: Engineering, Technology & Applied Sciences; EI Compendex Plus; Engineering Index; Geotechnical Abstracts; Health & Safety Science Abstracts; INSPEC; Metals Abstracts; Risk Abstracts.

Subscription Information 1996

For 1996 three volumes (22–24) are scheduled for publication. Back volumes and subscription prices are available on request. Subscriptions are accepted on a prepaid basis only and are entered on a calendar year basis. Issues are sent by SAL (Surface Air Lifted) mail wherever this service is available. Airmail rates are available upon request. Please address all enquiries regarding orders and subscriptions to:

Elsevier Science B.V.
Order Fulfilment Department
P.O. Box 211, 1000 AE Amsterdam
The Netherlands
Tel.: + 31 20 4853642, Fax: +31 20 4853598

Claims for issues not received should be made within six months of our publication (mailing) date.

US mailing notice - Mechanics of Materials (ISSN 0167-6636) is published monthly by Elsevier Science B.V., P.O. Box 211, 1000 AE Amsterdam, The Netherlands. Annual subscription price in the USA is US$ 876.00 (valid in North, Central and South America only), including air speed delivery. Second class postage rate paid at Jamaica, NY 11431.
USA POSTMASTERS: Send address changes to Mechanics of Materials, Publications Expediting, Inc., 200 Meacham Avenue, Elmont, NY 11003.
AIRFREIGHT AND MAILING in the USA by Publications Expediting, Inc., 200 Meacham Avenue, Elmont, NY 11003.

♾ The paper used in this publication meets the requirements of ANSI/NISO 239.48-1992 (Permanence of Paper).
Printed in The Netherlands

ELSEVIER

ELSEVIER

Mechanics of Materials 22 (1996) 51-64

MECHANICS OF MATERIALS

Number of grains required to homogenize elastic properties of polycrystalline ice

Alex A. Elvin

Massachusetts Institute of Technology, Department of Civil and Environmental Engineering, Room 5-330A, Cambridge, MA 02139, USA

Received 15 March 1995; revised version received 21 August 1995

Abstract

The number of grains required for homogeneous elastic behavior of polycrystalline $S2$ is determined in this paper. The two extreme cases of (i) no grain boundary slip and (ii) free grain boundary sliding are examined. Detailed finite element simulations of uniaxial loading of specimens containing polygonal grains are performed. The results show that at least 230 grains are required to homogenize the elastic properties. The effect of the grain's elastic anisotropy on the homogenized properties is more important when no grain boundary sliding is allowed; grain shape is more important when grain boundary sliding is permitted. The stress components at the grain centers approximately follow the Gaussian distribution. The average computed homogenized Young's modulus and Poisson ratio at $-16°C$ are: 9.58 GPa and 0.33 with no grain boundary sliding; 7.83 GPa and 0.45 with free grain boundary sliding.

Keywords: Representative area element; Polycrystalline ice; Homogenized elastic properties; Heterogeneous ensemble of anisotropic grains

1. Introduction

The homogeneous elastic properties of materials form an integral part of most constitutive theories, and are required in the solution of boundary value problems. In polycrystalline aggregates, crystallographic axes of neighboring grains are seldom aligned in the same direction. Hence there is a mismatch in elastic properties between neighboring grains in the global axes frame. Theoretical estimates of the elastic constants for polycrystals may be derived from the elastic properties of the constituent monocrystals. The theoretical elastic moduli for polycrystalline ice have been calculated by Michel (1978), Sinha (1989a), and Nanthikesan and Shyam Sunder (1994). These authors used one or more averaging assumptions of Voigt (1910) and Reuss (1929).

The method of Voigt (1910) assumes that all the grains undergo an uniform strain and thus an uniform stress. Thus on the scale of the grain, equilibrium is violated. The method of Reuss (1929), on the other hand, assumes a constant state of stress in all the grains. Thus, although equilibrium is preserved, adjacent grains may have different deformations leading to local violation of compatibility. Hill (1952) showed that the Voigt and Reuss (V-R) methods provide the upper and lower bounds of the elastic stiffness moduli. Other homogenization methods exist to calculate the effective moduli of polycrystals. Among these, for example, are the self-consistent and differential methods and the Hashin-Shtrikman bounds; the references for, and details of these and other methods are presented in Nemat-Nasser and Hori (1993). However, the work of Nanthikesan and Shyam Sunder (1994)

SSDI 0167-6636(95)00024-0

shows that the *maximum* discrepancy between the V-R bounds on the elastic moduli of columnar grained polycrystalline ice is only 4.2%. These authors conclude that the V-R bounds for polycrystalline ice are so close to each other and to experimental values, that either bound, or an average, can be used as the homogenized elastic moduli.

The fundamental assumptions behind the spatial averaging V-R methods is that the polycrystal contains a sufficient number of grains such that a *continuous* distribution of grain orientations exists. In reality, the number of grains in a polycrystal is finite. The aim of this paper is to quantify how many grains are required to ensure an elastically homogeneous response of polycrystalline ice. This number of grains specifies the size of the representative element. Two extreme idealized cases are considered: (i) neighboring grains are perfectly bonded to each other, i.e., no relative slip between the grains, and (ii) no shear stress transfer between neighboring grains, i.e., free grain boundary slip. Relative displacement between grains might be due to viscous effects, and/or due to a compliant grain boundary zone. The idealized case of no grain boundary slip approximates short duration, high loading rate, or high frequency tests. In both idealized cases the grains are assumed to remain elastic.

In this paper fresh water, columnar grained ice is considered. The c-axes of the individual crystals lie in the horizontal plane (the plane of the ice cover) and are randomly distributed. Hence the ice cover is transversely isotropic. This type of ice is found on lakes, and rivers with low flow velocities. Michel and Ramseier (1971) classified this ice type as $S2$. The nature of $S2$ ice allows for planar modeling of the polycrystalline aggregate. The behavior of ice can be ductile or brittle depending on the loading rate and temperature. The polycrystal deformation in the brittle regime, as well as the peak stresses at the high end of the ductile regime occurs at small strain ($< 1\%$).

In the present study, detailed finite element simulations of uniaxial loading of polycrystalline samples of various sizes are conducted. The grain geometry is modeled by modified Voronoi polygons (see Section 2.1). The grain's elastic anisotropy is specified in Section 2.2. The finite element model for the ensemble of grains is set up, and the homogenized elastic properties are defined in Sections 2.3 and 2.4, respectively. The experimental data on ice single crystal stiffness moduli used in the simulations is reported in Section 3. The results from the simulations of: (i) variation of homogenized elastic properties with number of grains, and (ii) the statistical distribution of residual stresses within the grains, are presented and discussed in Section 4.

2. The numerical model

The polycrystalline sample is idealized as an heterogeneous ensemble of randomly oriented, elastically anisotropic grains of random shape but approximately equal area. The two limits of (i) no grain boundary sliding and (ii) free grain boundary sliding are investigated. The primary aim in this study is to determine how many grains are required to ensure that the entire sample behaves isotropically. To this end, simulations of uniaxial loading of samples containing various numbers of grains are performed, and homogenized elastic properties are computed. This section describes how the grain geometry and elastic properties are set up, the computational model, and the method of homogenization.

2.1. Modeling the grain geometry

A cross section taken through columnar grained $S2$ ice perpendicular to the column axes, reveals grains that are approximately polygonal in shape and equal in area (see Sinha (1989b) for a typical section). The polygons are not regular and the number of facets varies from grain to grain. In the past, the grain geometry has been modeled effectively by Voronoi tessellation (sometimes refered to as Theissen or Dirichlet polygons), see for example Frost and Thompson (1987) who considered different conditions of grain nucleation and growth. In this paper the grains are represented by modified Voronoi polygons. The details and the motivation for the method by which grain geometry is constructed follows.

Standard Voronoi tessellation begins from a set of nucleation points, p. Next an unique triangulation grid involving the p points is constructed by Delaunay triangulation. Perpendicular bisectors of each side of the triangles are found. The intersections of the perpendicular bisectors form the vertices of the Voronoi polygons. One property of Voronoi polygons is that a point

lying anywhere within polygon P_i is closer to its nucleation point p_i then to any other nucleation point.

Since the grains in a section of *S*2 ice all have approximately the same area (see e.g., Sinha, 1989b) the nucleation points, p, cannot be distributed completely randomly on the plain. Instead, the points have to be constrained to lie a minimum distance apart, say $2r$; this requirement is met by placing rigid disks of diameter $2r$ *randomly* on the plain with no overlap, until no more will fit. This results in the polygons/grains having approximately the same area. This process still leads to facet lengths, l_i, which are very short compared to the distance from the nucleation point to the polygon vertex, Ve_i, i.e., $Ve_i \gg l_i$. These short facets result in numerical inaccuracies when solving for the stresses and strains within the grains. To obviate these difficulties the facets with $l_i/Ve_i < 0.3$ are lengthened. The vertices on either end of the short facet are shifted to:

$$V_j^{\mathrm{NEW}} = V_j^{\mathrm{OLD}} \frac{l_i}{Ve_i} \frac{1}{0.3} + c_j\left(1 - \frac{l_i}{Ve_i} \frac{1}{0.3}\right), \qquad (1)$$

where V_j is the coordinate of vertex j ($j = 1,2$), and c_j is the centroid coordinate of the corresponding triangle.

The specification of a sample size creates grain slivers on the boundaries as well as facets with $l_i/Ve_i < 0.3$; both lead to numerical difficulties. The short facets are removed by shifting the polygon vertices perpendicularly to the boundary. The grain slivers with nucleation points lying outside a strip of width $2r/2.5$, which surrounds the sample, are removed; the vertices of the neighboring polygons are moved perpendicularly to the boundary. Finally, the nucleation points of the polygons lying on the boundary are shifted to the polygons' geometric centers.

In all subsequent simulations $2r$ is set to 1 mm; thus approximately defining the average grain size. The area is defined only approximately due to the randomness in creating the grain geometry. Fig. 1a shows a 20×20 mm^2 sample with a typical grain geometry generated by the above process. The corresponding histogram of the grain areas is shown in Fig. 2a. The average grain area is 1.31 mm^2. As to be expected most grain areas cluster around the mean. The few grains which are slightly larger and slightly smaller are those found on the boundary. Their area differs from the mean due to the treatment of border grains described above.

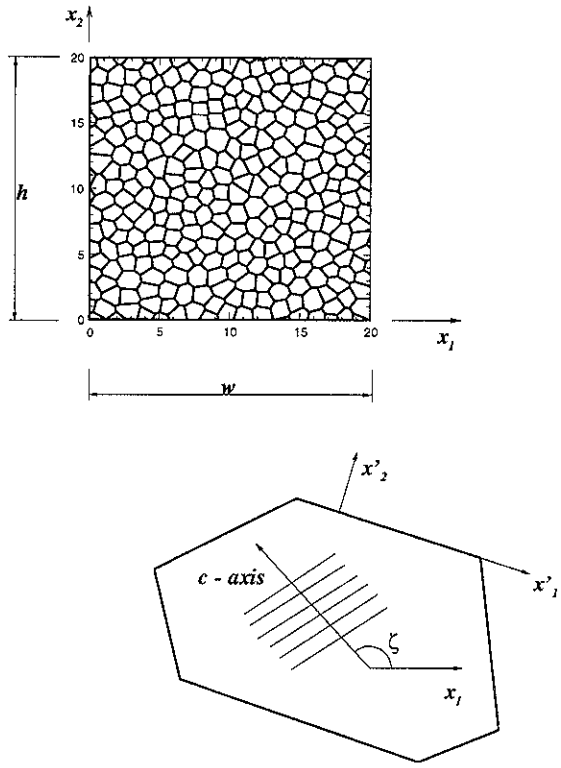

Fig. 1. (a) Typical grain geometry in a 20×20 mm^2 sample of 305 grains; (b) Typical grain with orientation ζ.

2.2. *The grain elastic properties*

Each grain in the polycrystalline aggregate is defined by its crystal orientation, here specified by the *c*-axis. The distribution of the *c*-axes in a macroscopically homogeneous and isotropic material is random. In the case of transversely isotropic *S*2 ice, the *c*-axes are randomly distributed in the plane of isotropy. The dynamic elastic stiffness tensor C_g^{3D} can be taken as constant for all the grains.

Since the overall macro-response of polycrystalline *S*2 ice is transversely isotropic with the plane of isotropy being the plane of interest, the three-dimensional C_g^{3D} can be reduced to plane conditions. Plane stress conditions are assumed since the ice

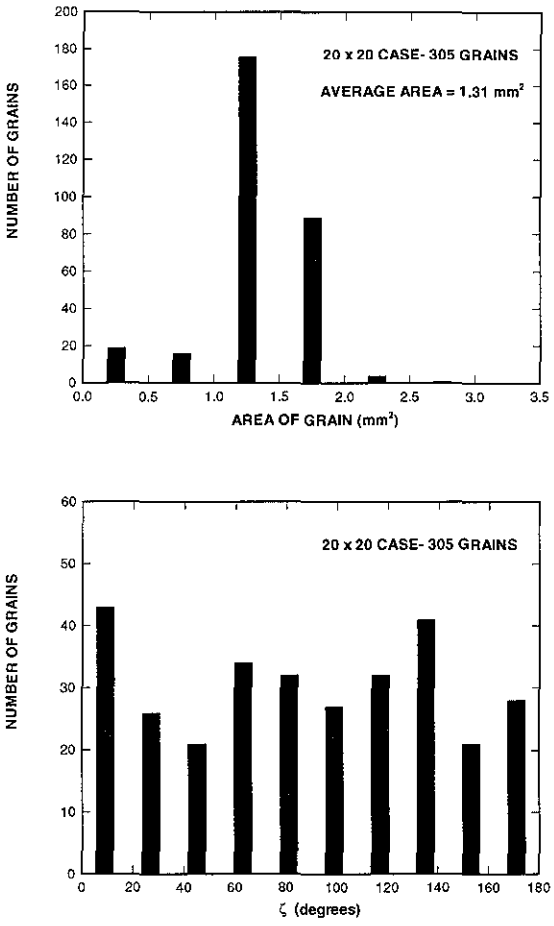

Fig. 2. Typical histograms for a 20×20 mm^2 sample of: (a) Grain area; (b) Grain orientation

plate thickness is much smaller than the in-plane $x_1 - x_2$ dimensions. This assumption modifies the single grain orthotropic stiffness tensor components $C_g^{3D}{}_{ij}$ as follows:

$$C_{g\,11} = C_g^{3D}{}_{11} - \frac{C_g^{3D}{}_{13}\; C_g^{3D}{}_{31}}{C_g^{3D}{}_{33}}$$

$$C_{g\,12} = C_g^{3D}{}_{12} - \frac{C_g^{3D}{}_{13}\; C_g^{3D}{}_{32}}{C_g^{3D}{}_{33}}$$

$$C_{g\,21} = C_g^{3D}{}_{21} - \frac{C_g^{3D}{}_{23}\; C_g^{3D}{}_{31}}{C_g^{3D}{}_{33}}$$

$$C_{g\,22} = C_g^{3D}{}_{22} - \frac{C_g^{3D}{}_{23}\; C_g^{3D}{}_{32}}{C_g^{3D}{}_{33}}$$

$$C_{g\,33} = C_g^{3D}{}_{33}\,. \tag{2}$$

In order to obtain the macroscopic behavior of the polycrystal, the components of $\boldsymbol{C}_g$ have to be determined in the global axes system. The components of $\boldsymbol{C}_g$ are usually specified in the axes system associated with the crystal lattice. The stiffness components in the global axes system are given by the standard fourth rank tensor transformation. In two dimensions this transformation can be expressed as:

$$\boldsymbol{C}_G = \boldsymbol{R}^{\mathrm{T}} \boldsymbol{C}_g \boldsymbol{R}\,, \tag{3}$$

where $\boldsymbol{C}_G$ contains the components of the grain stiffness in the global axes system, T is the transpose operation, and the transformation tensor $\boldsymbol{R}$ is given by:

$$\boldsymbol{R} = \begin{pmatrix} \cos^2(\zeta) & \sin^2(\zeta) & \frac{1}{2}\sin(2\zeta) \\ \sin^2(\zeta) & \cos^2(\zeta) & -\frac{1}{2}\sin(2\zeta) \\ -\sin(2\zeta) & \sin(2\zeta) & \cos(2\zeta) \end{pmatrix}. \tag{4}$$

The orientation of the grain is defined solely by ζ, the angle between the c-axis and the global x_1 direction (see Fig. 1b).

As indicated above, the c-axes are distributed uniformly in the $x_1 - x_2$ plane. Hence, in the numerical simulations each grain in the aggregate is associated with an orientation ζ which is chosen randomly from the range $0° \leq \zeta \leq 180°$. A typical histogram of uniformly distributed ζ is shown in Fig. 2b; this figure corresponds to the 20×20 mm^2 sample shown in Fig. 1a. Fig. 3 shows the grain geometries as well as the spatial distribution of ζ for various specimen sizes; notice the close resemblance with experimental observation of grain geometry reported in Sinha (1989b).

2.3. Computational model

The stress, strain and displacement fields in the heterogeneous assembly of grains are solved using the finite element method. Each grain is discretized into as many six-noded plane stress elements as there are facets in the grain. Fig. 4a shows a grain assembly and the corresponding discretization; a typical discretized grain is shown separately in Fig. 4b. Note that the elements do not straddle the grain boundaries. The anisotropic elastic material properties of each element

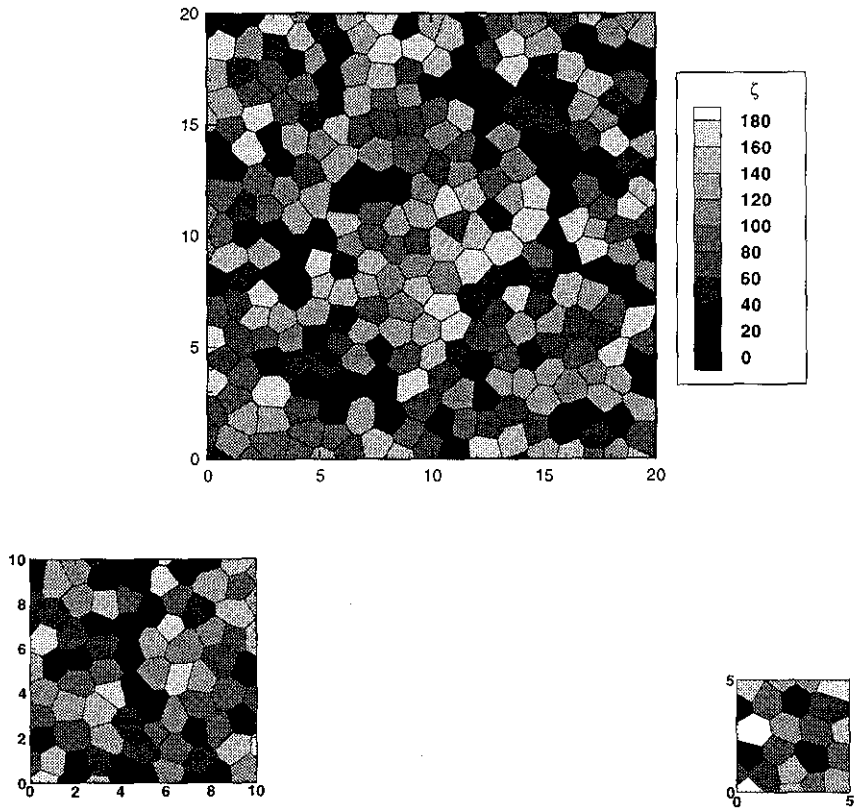

Fig. 3. Typical grain geometries and spatial distributions of grain orientation, ζ, for specimen size of: (a) 20×20 mm^2, (b) 10×10 mm^2, and (c) 5×5 mm^2

are assigned according to the grain orientation ζ and Eqs. (3) and (4).

The two limits of (i) no grain boundary sliding, and (ii) free grain boundary sliding are modeled as follows. In the coordinate axes of the grain facet $x_1' - x_2'$ (see Fig. 1b) constrain the displacement components, u_i':

For no grain boundary sliding:

$$u_1'^{+} = u_1'^{-} \quad \text{and} \quad u_2'^{+} = u_2'^{-} .$$

For free grain boundary sliding:

$$u_2'^{+} = u_2'^{-} , \tag{5}$$

where the + and − refer to two points lying infinitesimally close to, but on either side of, the grain bound-

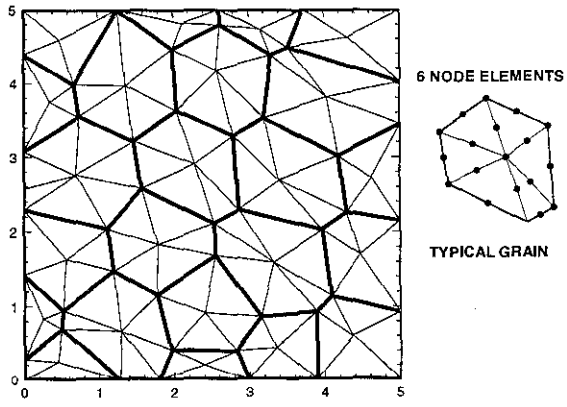

Fig. 4. (a) Typical grain assembly and the finite element discretization; (b) Detail of discretization of a typical grain.

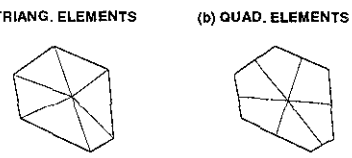

Fig. 5. Discretization of a typical grain with: (a) Triangular elements; (b) Quadrilateral elements.

ary. These constraints on the displacements are enforced by the penalty method.

To verify the fineness of the discretization the number of nodes is varied by changing the type and order of the elements: four- and eight-node quadrilateral elements, and three- and six-node triangular elements are considered. Discretizations of a typical grain with quadrilateral and triangular elements are shown in Fig. 5(a) and (b) respectively. The *global* convergence of the finite element discretization is quantified by the total strain energy, $\mathcal{E}$, of the aggregate:

$$\mathcal{E} = \tfrac{1}{2}\int_{\Omega} \boldsymbol{\sigma}\cdot\boldsymbol{\epsilon}\,\mathrm{d}\Omega = \frac{1}{2}\int_{\Gamma} \boldsymbol{P}\cdot\boldsymbol{u}\,\mathrm{d}\Gamma\,, \tag{6}$$

where $\boldsymbol{\sigma}$ and $\boldsymbol{\epsilon}$ are the stresses and strains, Ω is the total volume of the sample, $\boldsymbol{P}$ and $\boldsymbol{u}$ are tractions and displacements on the boundary Γ. In a typical case, with no grain boundary sliding, by increasing the number of nodes from 1167 (triangular three-node elements) to 5131 (eight-node quadrilaterals) decreases $\mathcal{E}$ by only 0.4%.[1] When grain boundary sliding is allowed, $\mathcal{E}$ varies as follows: 67.3, 61.4, 57.8, and 55.6 for 1167, 2158, 3149, and 5131 nodes, respectively. The variation in $\mathcal{E}$ by discretizing with six- versus eight-node elements is 4%. Thus using six-noded elements is more then acceptable when no grain boundary sliding is allowed and is satisfactory when grain boundary sliding is permitted. Note that the adopted discretization does not capture all the details in the stress field variation close to the grain triple points. However, since this paper is concerned with *homogenized* polycrystal behavior and since the zones of high stress variation are small, they have little effect on the sought solution and will be ignored.

[1] This particular specimen contains 176 grains; the sample size is 15×15 mm^2.

2.4. Homogenized elastic constants

The overall planar response of polycrystalline *S2* ice with a sufficient number of grains is isotropic. This material symmetry is fully characterized by two homogenized elastic constants: the homogenized Young's modulus, $\bar{E}$, and the homogenized Poisson ratio, $\bar{\nu}$. These parameters are determined from numerical simulations of a polycrystal sample subjected to uniaxial loading as follows.

Consider a rectangular, multi grain sample of width w and height h (see Fig. 1). The sample boundary $x_2 = 0$ is prevented from displacing; $u_2 = 0$. To ensure numerical stability one node on this boundary is also pinned. This allows unconstrained expansion/contraction in the x_1 direction on $x_2 = 0$. The sample is loaded uniaxially by applying an uniform displacement, u_2 all along the boundary $x_2 = h$.

The homogenized isotropic elastic constants are defined as:

$$\bar{E} = \frac{\bar{\Sigma}_2}{\bar{\epsilon}_2} \quad \text{and} \quad \bar{\nu} = -\frac{\bar{\epsilon}_1}{\bar{\epsilon}_2}\,, \tag{7}$$

where the average quantities are:

Average normal strain components in x_1 and x_2 directions:

$$\bar{\epsilon}_1 = \frac{1}{w}\int_0^h \frac{u_1(x_1 = w, x_2) - u_1(x_1 = 0, x_2)}{h}\,\mathrm{d}x_2$$

$$\bar{\epsilon}_2 = \frac{1}{h}\int_0^w \frac{u_2(x_1, x_2 = h) - u_2(x_1, x_2 = 0)}{w}\,\mathrm{d}x_1\,. \tag{8}$$

Average normal stress component in x_2 direction:

$$\bar{\Sigma}_2 = \int_0^w \frac{T_2}{w}\,\mathrm{d}x_1 = \sum \frac{R_2(x_2 = h)}{w\,t}\,, \tag{9}$$

where T_2 is the traction component in the x_2 direction. Note that $\bar{\Sigma}_2$ is most easily obtained from the finite element solution by summing all the nodal reaction components $R_2(x_2 = h)$ on the boundary $x_2 = h$ and dividing by the sample width w and thickness t.

3. Material properties

The values for the dynamic elastic moduli of ice single crystals are reported in the literature. The data of Dantl (1969) and Gammon et al. (1983) are the most comprehensive and accurate available to date. The maximum difference between the elastic stiffness components of these two data sets is 5.45 % at −16°C. The reported uncertainty in the stiffness data of Gammon et al. (1983) is less than in Dantl (1969): the maximum uncertainty is ±0.46% in the data of Gammon et al. (1983) and ±7% in the data of Dantl (1969). Further, as pointed out by Nanthikesan and Shyam Sunder (1994) the stiffness and compliance data of Gammon et al. (1983) satisfies the inverse relationship, while the data of Dantl (1969) does not. Although using the stiffness data from either reference will have little effect on the present results, in view of the above, the data of Gammon et al. (1983) are used in the simulations.

The dynamic elastic stiffness of a single ice crystal, measured using Brillouin spectroscopy at −16°C is reported in Gammon et al. (1983):

$$\boldsymbol{C}_{\mathrm{g}}^{3\mathrm{D}}(\zeta = 0^\circ) = \begin{pmatrix} 15.010 & 5.765 & 5.765 & & & \\ & 13.929 & 7.082 & & 0 & \\ & & 13.929 & & & \\ & & & 3.4235 & & \\ & \text{sym.} & & & 3.014 & \\ & & & & & 3.014 \end{pmatrix} \text{GPa}, \tag{10}$$

where in the grain's axes system, $x_2 - x_3$ is the isotropy plane in the transversely isotropic crystal; the c-axis lies in the x_1 direction ($\zeta = 0^\circ$). The above elastic constants are mildly temperature dependent. The following empirical relationship for the stiffness at temperature T is presented in Gammon et al. (1983):

$$\boldsymbol{C}_{\mathrm{g}}^{3\mathrm{D}}(T) = \boldsymbol{C}_{\mathrm{g}}^{3\mathrm{D}}(T_{\mathrm{ref}})\,\frac{(1 - 1.418 \times 10^{-3}T)}{(1 - 1.418 \times 10^{-3}T_{\mathrm{ref}})}, \tag{11}$$

where T_{ref} is the temperature at which $\boldsymbol{C}_{\mathrm{g}}^{3\mathrm{D}}$ is known ($T_{\mathrm{ref}} = -16^\circ\mathrm{C}$), and all temperatures are measured in degrees Celsius. Eq. (11) shows that between 0°C and −20°C the variation in dynamic stiffness of a single crystal is practically negligible.

Reducing the single crystal stiffness, Eq. (10), to plane stress conditions by using Eq. (2), with $\sigma_{33} = 0$ and $x_1 - x_2$ being the plane of interest, the following is obtained:

$$\boldsymbol{C}_{\mathrm{g}}(\zeta = 0^\circ) = \begin{pmatrix} 12.624 & 2.832 & 0 \\ 2.832 & 10.328 & 0 \\ 0 & 0 & 3.014 \end{pmatrix} \text{GPa}. \tag{12}$$

In all subsequent simulations these stiffness moduli are used.

4. Results and discussion of numerical simulations

4.1. Number of grains required to homogenize elastic properties

This section presents and discusses the results from simulations of uniaxial loading of polycrystalline ice specimens. Both limits of (i) no grain boundary sliding, and (ii) free grain boundary sliding are investigated. Only square samples ($h = w$ in Fig. 1a) are analyzed. The following seven specimen sizes, $h \times h$, are considered: 5×5 mm^2, 7.5×7.5 mm^2, 10×10 mm^2, 12.5×12.5 mm^2, 15×15 mm^2, 17.5×17.5 mm^2, and 20×20 mm^2. Three typical specimens, all different in size, are shown in Fig. 3.

By choosing different seeds for the random number generator, different grain geometries are created for the same sample size, $h \times h$. The orientations of the grains, ζ, which effects the grains elastic properties in the global axes frame, are also re-randomized. Simulations with at least 25 different grain geometries and orientations, for each of the first four sample sizes, are performed. For each of the remaining larger samples, simulations with at least 30 different random grain geometries are conducted. Note that due to the method of generating the grain geometry (see Section 2.1) the number of grains in a $h \times h$ size sample is not constant. The number of simulations conducted for each sample size is thought to provide a good indication of the variation in the homogenized elastic properties.

The effect of elastic anisotropy in the $h \times h$ sample is studied by randomly varying only the grain orientations, ζ. The grain geometry is held constant for each $h \times h$ sample. The same number of simulations are performed for each sample size as reported above.

The results presented below are independent of grain size. This was verified by generating self-similar samples, each composed of different mean grain size, i.e., the grain tessellation for the different sized samples was identical. The computed homogenized elastic properties were the same for the different self-similar specimens. This observation is not surprising. In the uniaxial loading simulations, the stress fields depend on the length scale only near the triple points where the solution is singular. For ice, the singularities at the triple points are relatively weak (see, e.g., Gupta et al., 1993). Hence the region effected by the singularities are small compared with the grain area and have little influence on the homogenized parameters sought.

It is interesting to note that in the self-consistent method averaging only a small number of crystals gives accurate overall moduli. For example, Iwakuma and Nemat-Nasser (1984) calculated the overall moduli of a polycrystal solid, subject to finite elasto–plastic deformation, and needed only 46, or fewer, grain orientations (this corresponds to a sample smaller than 7.5×7.5 mm^2). These authors add a cautionary note that at large strains (presumably where the mismatch between grains has developed substantially) the overall behavior depends on the number of grains considered. The following question arises: will the number of grains required in the self-consistent method suffice to homogenize the elastic properties when the polycrystal is viewed as an assembly of individual grains? In the self-consistent method, the following auxiliary problem is solved first: a homogeneous matrix which possess the average macroscopic moduli with an embedded single grain (usually circular or ellipsoidal in shape) is subjected to nominal macroscopic loading. Subsequently, the overall and single crystal moduli are related by averaging over all crystal orientations and shapes. The assumption in the self-consistent method that each crystal is surrounded by an equivalent *homogeneous matrix* is valid only if a sufficient number of grains surround the given crystal. An indication of this number is provided by Laws and Lee (1989): these authors calculate that at least 200 grains are required for accurate residual stress fields when the polycrystal is subject to a temperature drop.[2] Thus the number of grains required to homogenize the elastic properties is expected to be greater than in the self-consistent scheme.

[2] Laws and Lee (1989) considered regular hexagonal grains which were elastically isotropic but thermally anisotropic.

4.1.1. Effect of temperature

Changing the temperature has the same effect on all the components of the single crystal moduli, see Eq. (11). Since linear elastic behavior is considered, having the solution at a certain temperature, T_{ref}, the solution at a new temperature T can be scaled using Eq. (11). In particular, the homogenized Young's modulus at a temperature T, $\bar{E}(T)$, is given by:

$$\bar{E}(T) = \bar{E}(T_{\text{ref}}) \frac{(1 - 1.418 \times 10^{-3} T)}{(1 - 1.418 \times 10^{-3} T_{\text{ref}})} . \tag{13}$$

The homogenized Poisson ratio should be unaffected by a temperature change, since:

$$\bar{\nu} = \frac{\bar{E}(T)}{2\bar{G}(T)} - 1 , \tag{14}$$

where $\bar{G}$ is the homogenized shear modulus, and the thermal effects on $\bar{E}(T)$ and $\bar{G}(T)$ are the same and hence cancel each other. Some evidence of the Poisson ratio independence of temperature has been observed experimentally by Langleben and Pounder (1963), in the -3.6°C to -15°C range, albeit for sea ice. However, Sinha (1989b) observes that there is little discrepancy in the reported dynamic Poisson ratio of different ice types.

4.1.2. No grain boundary sliding

The homogenized elastic properties can be calculated by the spatial averaging methods of Voigt (1910) and Reuss (1929) (as done by Nanthikesan and Shyam Sunder, 1994; Sinha, 1989a; Michel, 1978). As mentioned in the introduction, Hill (1952) showed that the Voigt and Reuss (V-R) limits give the upper and lower bound solutions for the aggregate stiffness moduli. Nanthikesan and Shyam Sunder (1994) calculate the V-R limits for the elastic properties of *S2* ice in the plane of isotropy and at -16°C to be:

$$9.726 \geq \bar{E} \geq 9.431$$

$$0.320 \leq \bar{\nu} \leq 0.334 \tag{15}$$

Figs. 6a and 6b plot the homogenized Young's modulus, $\bar{E}$, and Poisson ratio $\bar{\nu}$ versus the number of grains obtained from the simulations with no grain

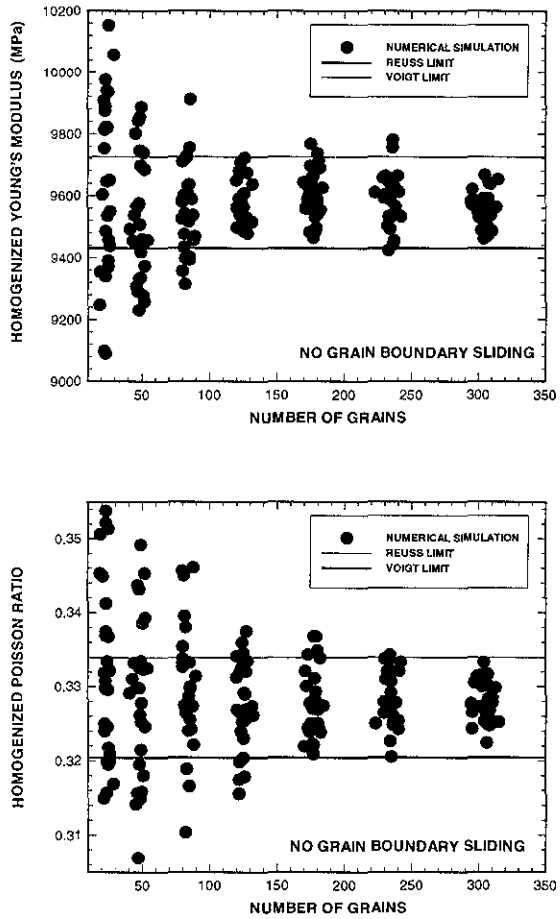

Fig. 6. (a) Homogenized Young's modulus, $\bar{E}$, versus number of grains; (b) Homogenized Poisson ratio, $\bar{\nu}$, versus number of grains. No grain boundary sliding; both grain geometry and grain orientation varied.

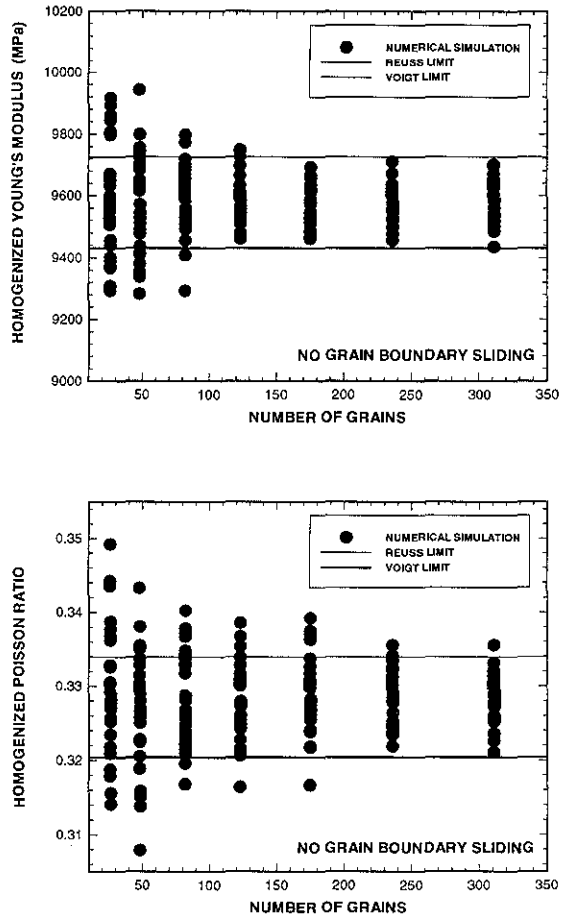

Fig. 7. (a) Homogenized Young's modulus, $\bar{E}$, versus number of grains; (b) Homogenized Poisson ratio, $\bar{\nu}$, versus number of grains. No grain boundary sliding; only grain orientation varied.

boundary sliding. In this figure both the grains geometry and orientations are varied. The V-R upper and lower bounds given in Eq. (15), are also plotted. Figs. 6a and 6b show that as the number of grains increase so the band of simulated homogenized properties decreases, and then reaches approximately a constant width. For sample sizes larger than 17.5×17.5 mm^2, the bands of homogenized properties produced by the simulations are very close to the V-R band.

The effect of grain anisotropy is studied in Figs. 7a and 7b, by varying only the grain orientations and keeping the grain geometry fixed. No grain boundary sliding is allowed. The bands produced by varying only ζ are wider than varying both grain geometry and orientations. Thus when there is no grain boundary sliding, the effect of grain anisotropy is greater than the effect of grain shape.

The minimum, average and maximum values of the homogenized elastic properties from all the simulations are reported in Table 1. The percentage difference between the maximum and minimum values are also given. From Table 1 it can be seen that the homogenized Poisson ratio converges slower than the Young's modulus. The averages of $\bar{E}$ and of $\bar{\nu}$ for dif-

Table 1
Statistics for homogenized Young's Modulus and Poisson ratio for various numbers of grains; no grain boundary sliding allowed; all simulations considered.

Sample Size (mm^2)	$\bar{E}$ (MPa)				$\bar{\nu}$			
	Min.	Ave.	Max.	% Diff.	Min.	Ave.	Max.	% Diff.
5×5	9090	9604	10153	11.7	0.291	0.329	0.354	21.72
7.5×7.5	9231	9549	9943	7.71	0.307	0.328	0.349	13.77
10×10	9293	9581	9912	6.67	0.310	0.329	0.346	11.52
12.5×12.5	9461	9582	9750	3.05	0.316	0.328	0.339	7.28
15×15	9462	9584	9769	3.24	0.317	0.328	0.339	7.12
17.5×17.5	9425	9576	9781	3.78	0.321	0.328	0.336	4.69
20×20	9436	9566	9702	2.83	0.321	0.328	0.336	4.52

ferent sample sizes are all approximately the same. This is due to the *random* variation of the grain geometry and grain shape. Table 1 shows that samples larger than 17.5 × 17.5 mm^2 produce bands narrower than 5% and which are very close to the V-R bounds. Note that the simulations conducted here are by no means exhaustive; however, the results indicate that a sample of 17.5 × 17.5 mm^2, or approximately 230 grains, serves as a representative area of the polycrystal.

Experimental data on the Young's modulus and Poisson ratio for polycrystalline ice are available in the literature. Gold (1958) tabulates results of the sonic values of Young's modulus and Poisson ratio at −5°C. The reported values for the Young's modulus range from 8.95 GPa to 9.94 GPa; the Poisson ratio ranges from 0.31 to 0.365. Sinha (1978) measured the Young's modulus of polycrystalline *S2* ice in the plane of isotropy, at temperatures between −40°C and −45°C, and reports a range of 9.1–9.8 GPa with an average of 9.3 GPa. More recently, the Poisson ratio was measured by Sinha (1989b) at −20°C to be 0.31–0.32. The numerical simulations on 17.5 × 17.5 mm^2 samples predict the Poisson ratio to lie in the range 0.32–0.34. The average homogenized Young's modulus, corrected for temperature according to Eq. (13), are: at −5°C, $\bar{E}$ = 9.43 GPa, and at −40°C, $\bar{E}$ = 9.89 GPa. The simulated values are in agreement with experimental measurements.

4.1.3. Grain boundary sliding

The results presented in this section are from simulations with free grain boundary sliding. In Figs. 8a and 8b the homogenized Young's modulus, $\bar{E}$, and Poisson ratio $\bar{\nu}$ are plotted versus the number of grains in the sample; both the grains geometry and orientations are varied. The effect of elastic anisotropy is studied in Figs. 9a and 9b, where only the grain orientations are varied, for a single grain geometry. The results from all these simulations are presented in Table 2.

As to be expected, as the number of grains increases so the bands in the homogenized elastic properties decreases. For samples bigger than 17.5 × 17.5 mm^2, i.e. samples containing more than 230 grains, the bands' widths approximately stabilize. Note that the grains on the specimen border are relatively unconstrained, and due to *free* grain boundary slip, are almost unloaded. Hence in the smaller samples, where the number of grains on the border is a large fraction of the total number of grains, large variability is seen in the homogenized elastic properties.

The bands formed by varying only the grain orientations (Figs. 9a and 9b) are much narrower than when both the grain geometry and the orientations are varied (Figs. 8a and 8b). Thus grain shape is more important than elastic anisotropy when grain boundary sliding occurs. This conclusion is in contrast to the case of no grain boundary sliding, where elastic anisotropy is more dominant in producing the variability in the polycrystal elastic constants.

Sinha (1989b) measured the effective Young's modulus and Poisson ratio of fresh water polycrystalline *S2* ice at −20°C. His results show that the Poisson ratio decreases monotonically from about 0.7 to 0.3 as the strain rate varies from 10^{-7} s^{-1} to 10^{-2} s^{-1}. The effective Young's modulus increased from 4 GPa to approximately 9.5 GPa. Gold (1958) also reports data from experiments conducted on the

Table 2
Statistics for homogenized Young's Modulus and Poisson ratio for various numbers of grains; free grain boundary sliding permitted; all simulations considered.

Sample Size (mm^2)	$\bar{E}$ (MPa)				$\bar{\nu}$			
	Min.	Ave.	Max.	% Diff.	Min.	Ave.	Max.	% Diff.
5×5	6687	7408	8306	24.22	0.412	0.475	0.503	22.11
7.5×7.5	6947	7815	8148	17.29	0.425	0.456	0.560	31.83
10×10	7246	7738	8182	12.91	0.417	0.463	0.526	26.06
12.5×12.5	7300	7738	8076	10.64	0.430	0.455	0.487	13.32
15×15	7337	7765	8184	11.54	0.425	0.453	0.479	12.86
17.5×17.5	7526	7828	8060	7.10	0.433	0.447	0.473	9.15
20×20	7620	7827	7997	4.95	0.430	0.450	0.466	8.63

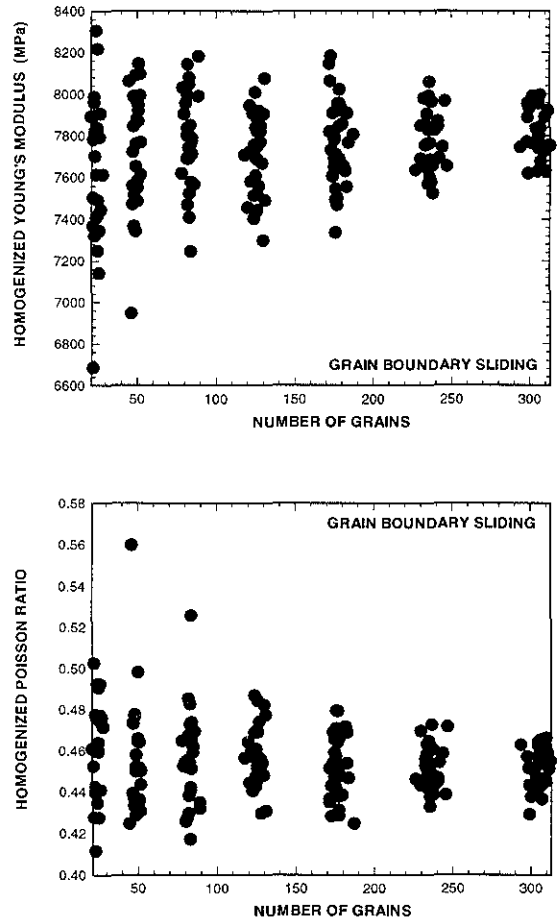

Fig. 8. (a) Homogenized Young's modulus, $\bar{E}$, versus number of grains; (b) Homogenized Poisson ratio, $\bar{\nu}$, versus number of grains. Free grain boundary sliding; both grain geometry and grain orientation varied.

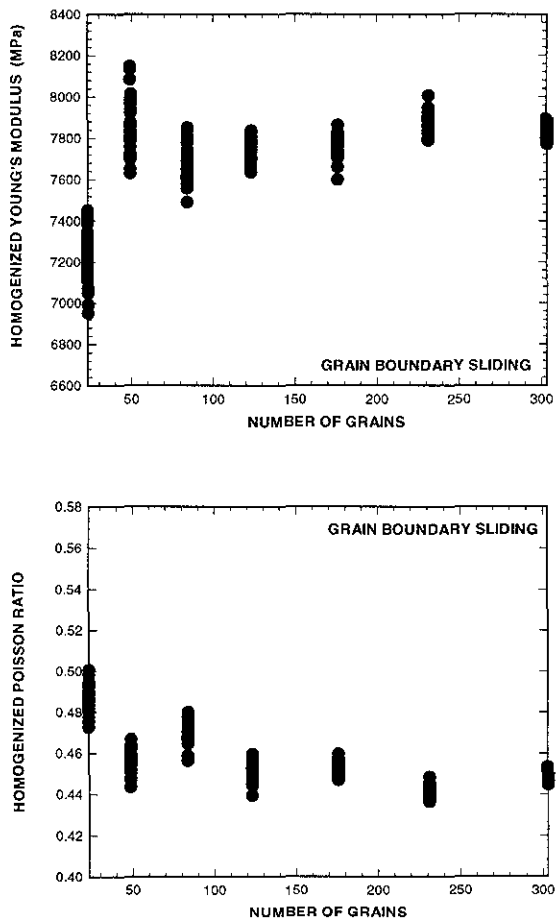

Fig. 9. (a) Homogenized Young's modulus, $\bar{E}$, versus number of grains; (b) Homogenized Poisson ratio, $\bar{\nu}$, versus number of grains. Free grain boundary sliding; only grain orientation varied.

same type of ice, but under static loading conditions; his results indicate Poisson ratio values of 0.31–0.54. In both these references the stress was restricted to low levels where the deformation was homogeneous and elastic; both references reason that grain boundary slip plays a role in the observed strains. The average elastic parameters obtained from the simulations when grain boundary sliding is allowed, are: $\bar{E} = 7.9$ GPa and $\bar{\nu} = 0.45$. These simulated values are in accord with the above experimental observations. The predicted elastic properties correspond to the strain range $10^{-4}s^{-1} - 10^{-3}s^{-1}$ in the data of Sinha (1989b). This strain range corresponds to the ductile to brittle transition in polycrystalline ice where maximum compressive stresses are observed.

4.2. Statistical distribution of stress at grain centers

Due to the elastic mismatch between neighboring crystals, residual stresses are set up within the grains when the polycrystal is loaded. Ortiz and Suresh (1993) have shown that the residual stresses within a polycrystal ceramic, subject to thermal cooling, follow the Gaussian distribution. They considered an array of regular hexagonally shaped grains, with elastic and thermal anisotropy, and no grain boundary slip. This section extends the work of Ortiz and Suresh (1993). The statistical distribution of stresses when a polycrystal of non-regular shaped grains subject to uniaxial loading is presented; both no grain boundary sliding and free grain boundary sliding are considered.

The probability distributions of the stress components for two typical 20×20 mm^2 samples, one without grain boundary sliding, and the other with free grain boundary sliding, are plotted in Figs. 10 and 11, respectively. The stresses only at the grain centers are considered. The magnitude of the stress components are normalized by the applied uniaxial stress; since the specimen is loaded by a displacement, u_2 (see Section 2.4), the equivalent normalizing stress is given by $|\bar{E}u_2/h|$. In addition, Gaussian distributions, or normal curves are fitted to the simulated normalized stress components. The Gaussian curves require the mean stress component, $\bar{\sigma}_i$, and the standard deviation, s_i:

$$\bar{\sigma}_i = \frac{1}{N}\sum_{j=1}^{N}(\sigma_i^*)_j$$

$$s_i^2 = \frac{1}{N}\sum_{j=1}^{N}((\sigma_i^*)_j - \bar{\sigma}_i)^2 , \tag{16}$$

where N is the number of grains in the specimen, and σ_i^* is the normalized stress component i.

The stress components in a polycrystalline aggregate approximately follow the Gaussian distribution; as observed by Ortiz and Suresh (1993) in hexagonal grains. When no grain boundary sliding is permitted (Fig. 10), the lateral $\bar{\sigma}_1$ and shear $\bar{\sigma}_3$ have zero mean stress components. In the uniaxial direction on the other hand, $\bar{\sigma}_2$, the mean normalized stress is -1; the negative sign indicates that the applied displacement loading, u_2 caused uniaxial *compression*. These results are to be expected since equilibrium has to be maintained.

When free grain boundary sliding is allowed, the grains on the sample boundary are unconstrained, and hence unloaded relative to the grains within the sample. The specimen boundary grains bias the stress distributions, and hence these grains are excluded in Fig. 11. The distributions for the free grain boundary slip case are also approximately Gaussian. Note however, while the mean shear stress component $\bar{\sigma}_3$ is once again zero, the other mean components, $\bar{\sigma}_1 \neq 0$ and $\bar{\sigma}_2 \neq -1$. The mean stresses are not the same as in the no grain boundary sliding case because of two effects. First, due to the applied uniaxial compression and grain boundary slip, at each grain triple point, one grain wedges the other two grains apart. This results in: (i) the wedging grain having a locally high *compressive* σ_2 component, and (ii) the other two grains having locally high *tensile* σ_1 components. Second, since the stress components are sampled only at the grain centers, instead of taking a volume average, the wedging effect is not canceled out. Hence, the mean lateral normalized stress component is tensile, $\bar{\sigma}_1 > 0$ while the mean axial component $\bar{\sigma}_1 < -1$. The local grain wedging action, causing locally tensile σ_1 fields, has significant implications for microcracking in polycrystalline ice loaded in compression (see Elvin and Shyam Sunder (1994) for details).

5. Conclusion

This paper examines how many grains are required to homogenize the elastic behavior of polycrystalline

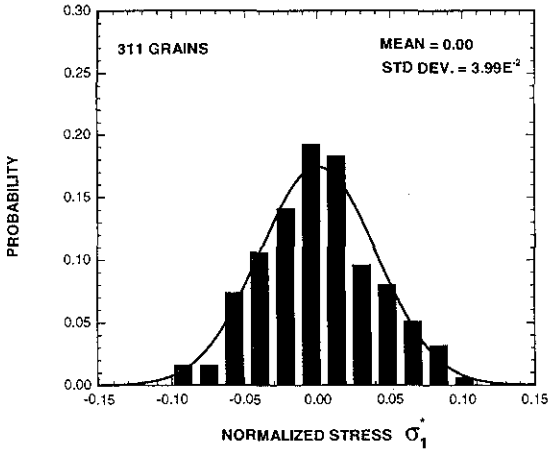

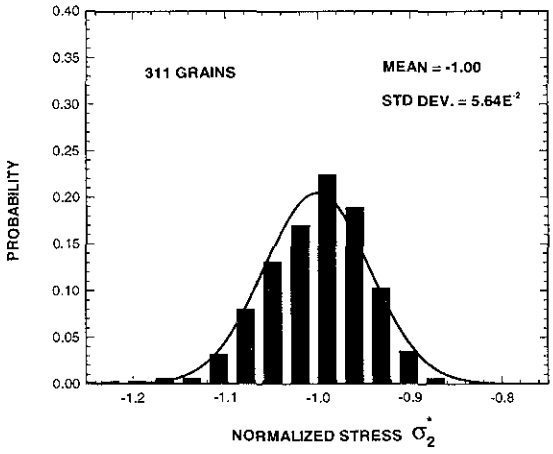

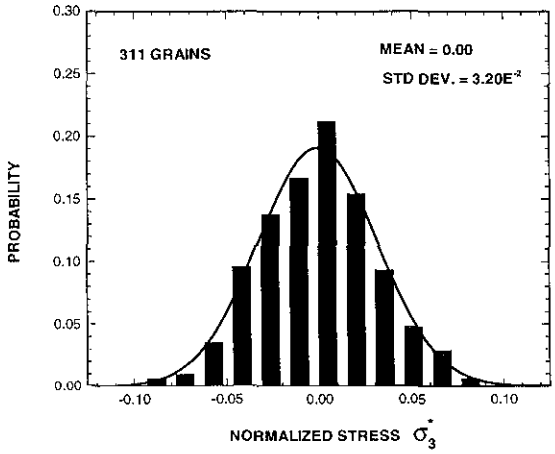

Fig. 10. Distribution of stress components at the grain centers; no grain boundary sliding. Solid lines represent Gaussian fits.

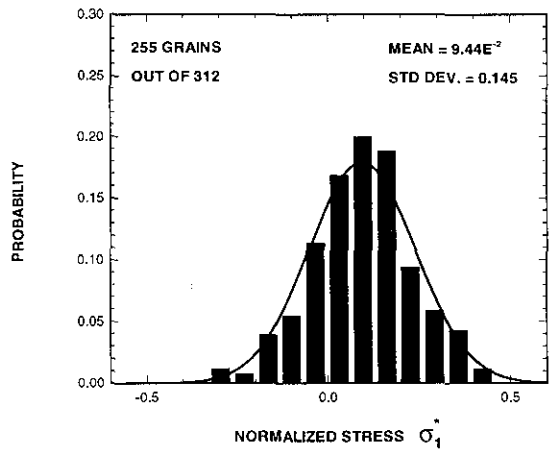

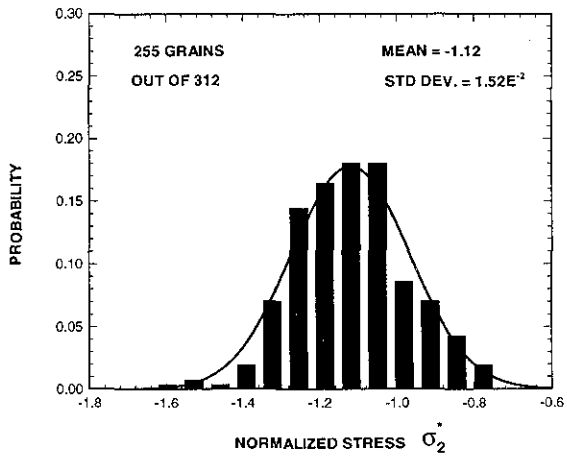

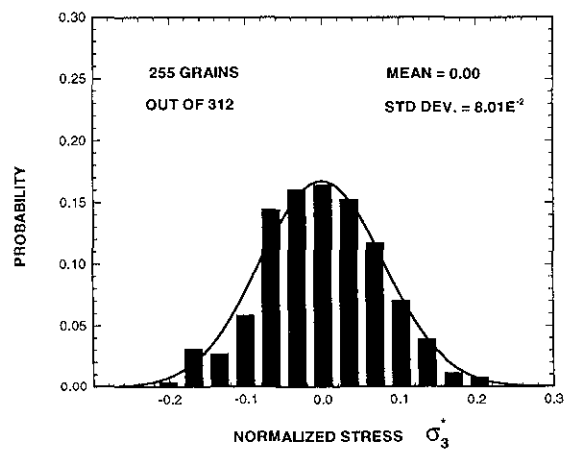

Fig. 11. Distribution of stress components at the grain centers; free grain boundary sliding. Solid lines represent Gaussian fits

S2 ice. Two extreme limits are considered: (i) no grain boundary sliding, and (ii) free grain boundary slip. The grain geometry is modeled by modified Voronoi polygons. The elastic anisotropy of the grains is accounted for. Finite element simulations of uniaxial compression of various size specimens are conducted.

Results show that at least 230 grains are required in order for the polycrystal aggregate to exhibit homogenized elastic behavior. When no grain boundary sliding is allowed, numerically computed homogenized Young's modulus and Poisson ratio bands are very close to the Voigt and Reuss theoretical upper and lower bounds. The effect of grain anisotropy on the homogenized elastic constants is more important then grain shape when no grain boundary sliding is allowed. The effect of grain shape on the homogenized properties is dominant when free grain boundary sliding occurs. The average computed homogenized Young's modulus and Poisson ratio are: 9.58 GPa and 0.33 with no grain boundary sliding; 7.83 GPa and 0.45 with free grain boundary sliding. The stress components at the grain centers approximately follow a Gaussian distribution. The same distribution was calculated by Ortiz and Suresh (1993), but for an array of hexagonal grains subject to thermal loading and with no grain boundary sliding.

The 230 grains required to homogenize the elastic response of the polycrystal defines the representative area element. At least this number of grains has to be considered when conducting micromechanical studies on polycrystalline *S2* ice. On the other hand, the resolution in large scale boundary value problems, with homogeneous constitutive laws (e.g., in-plane indentation of a floating ice sheet) especially in regions of high stress fluctuation, cannot be finer than this representative area element.

Acknowledgements

The comments of Prof. Nemat-Nasser and the helpful suggestions of N. Elvin are acknowledged. This research was supported by the Office of Naval Research (Grant No. N00014-92-J-1208) and by Minerals Management Service (Contract No. 14-35-0001-30735).

References

Dantl, G. (1969), Elastic Moduli of Ice, in: N. Rielhl, B. Bullemer and H. Engelhardt, eds., *Physics of Ice*, Plenum Press, New York, p. 223.

Elvin, A.A. and S. Shyam Sunder (1994), Microcracking due to grain boundary sliding in polycrystalline ice under uniaxial compression, *Acta Metall. Mater.*, in press.

Frost, H. J. and C.V. Thompson (1987), The Effect of nucleation conditions on the topology and geometry of two-dimensional grain structures, *Acta Metall. 35*, 529.

Gammon, P.H., H. Kiefte, M.J. Clouter and W.W. Denner (1983), Elastic constants of artificial and natural ice samples by Brillouin spectroscopy, *J. Glaciol. 29*, 433.

Gold, L.W. (1958), Some observations on the dependence of strain on stress for ice, *Can. J. Phys. 36*, 1265.

Gupta, V., R.C. Picu and H.J. Frost (1993), Crack nucleation mechanism in saline ice, *Ice Mechanics*, in: J.P. Dempsey, Z.P. Bazant, Y.D.S. Rajapakse and S.S. Sunder, eds., ASME, AMD, 163, p. 199.

Hill, R. (1952), The elastic behavior of a crystalline aggregate, *Proc. Phys. Soc. A 65*, 349.

Iwakuma, T. and S. Nemat-Nasser (1984), Finite elastic–plastic deformation of polycrystalline metals, *Proc. R. Soc. Lond. A 394*, 87.

Langleben, M. P. and E.R. Pounder (1963), Elastic parameters of sea ice, in: W.D. Kingery, ed., *Ice and Snow*, MIT Press, Cambridge, MA, p. 69.

Laws, N. and J.C. Lee (1989), Microcracking in polycrystalline ceramics: elastic isotropy and thermal anisotropy, *J. Mech. Phys. Solids 37*, 603.

Michel, B. and R.O. Ramseier (1971), Classification of river and lake ice, *Can. Geotech. J.*, 8, 36.

Michel, B. (1978), The strength of polycrystalline ice, *Can. J. Civil Eng. 5*, 285.

Nanthikesan, S. and S. Shyam Sunder (1994), Anisotropic elasticity of polycrystalline ice I_h, *Cold Reg. Sci. Technol. 22*, 149.

Nemat-Nasser, S. and M. Hori (1993), *Micromechanics: Overall Properties of Heterogeneous Materials*, Elsevier, Amsterdam.

Ortiz, M. and S. Suresh (1993), Statistical properties of residual stresses and intergranular fracture in ceramic materials, *J. Appl. Mech. 60*, 77.

Reuss, A.Z. (1929), Berechnung der Fließgrenze von Mischkristallen auf Grund der Plastizitätsbedingung fur Einkristalle, *Z. Angew. Math. Mech. 9*, 49.

Sinha, N.K. (1978), Rheology of columnar-grained ice, *Exp. Mech.*, 18, 464.

Sinha, N.K. (1989a), Elasticity of natural types of polycrystalline ice, *Cold Reg. Sci. Technol. 17*, 127.

Sinha, N.K. (1989b), Experiments on anisotropic and rate-sensitive strain ratio and modulus of columnar-grained ice, *J. Offshore Mech. Arc. Eng. 111*, 354.

Voigt, W. (1910), *Lehrbuch Der Krystallphysik*, Teubner, Berlin.

MECHANICS OF MATERIALS

Instructions to Authors

Submission of papers
Manuscripts (one original + two copies), accompanied by a covering letter, should be sent to either the editor-in-chief or to the co-editor indicated on page 2 of the cover.
Original material. It is the editorial policy of Mechanics of Materials that all manuscripts submitted for possible publication in the journal should be accompanied by a statement by the authors indicating: (a) Whether or not the paper is concurrently submitted for publication elsewhere. (b) Whether the paper, in its entirety, in part, or in a modified version, has been published elsewhere. If so, please supply pertinent information. (c) Whether or not the paper has previously been submitted for possible publication elsewhere and was subsequently rejected or withdrawn. In either case, please supply relevant information.
Refereeing Procedure. All contributions are reviewed expeditiously but thoroughly. In most cases, reliance will be placed on local reviewers so that the time for the review is reduced to usually three weeks, and certainly no more than two months, after receipt of the manuscript. In exceptional circumstances, where comments by several outside reviewers become necessary, the author will be consulted no later than three weeks after receipt of the manuscript.

Types of contributions
Mechanics of Materials contains research papers, invited review articles, brief notes, letters to the editor, book reviews, and some pertinent scientific items.

Manuscript preparation
All manuscripts should be written in good English. The use of metric units of the SI (Système Internationale) form is obligatory. The paper copies of the text should be prepared with double line spacing and wide margins, on numbered sheets. See notes opposite on electronic version of manuscripts.
Structure. Please adhere to the following order of presentation: Article title, Author(s), Affiliation(s), Abstract, Keywords, Main text, Acknowledgements, Appendices, References, Figure captions, Tables.
Corresponding author. The name, complete postal address, telephone and fax numbers and the e-mail address of the corresponding author should be given on the first page of the manuscript.
Keywords. Please supply 6–8 keywords of your own choice for indexing purposes.
References. Must be cited in the text according to the Harvard name/year convention, i.e. listing the names of the authors with the publication date placed in parentheses, e.g., Bishop and Hill (1951) or (Armstrong, 1953; Bishop and Hill, 1951). The cited references should be listed in alphabetical order at the end of the article. Each reference should include: names of authors, year of publication (in parentheses), title, abbreviated journal title, volume number, and the page numbers. For books, the publisher should be given.

Illustrations
Illustrations should also be submitted in triplicate: one master set and two sets of copies. The *line drawings* in the master set should be original laser printer or plotter output or drawn in black india ink, with careful lettering, large enough (3–5 mm) to remain legible after reduction for printing. Complex diagrams should be referred to as figures and should be numbered consecutively; simple diagrams can be typeset. The *photographs* should be originals, with somewhat more contrast than is required in the printed version. They should be unmounted unless part of a composite figure. Any scale markers should be inserted on the photograph, not drawn below it.
Colour plates. Figures may be published in colour, if this is judged essential by the Editor. The Publisher and the author will each bear part of the extra costs involved. Further information is available from the Publisher.

After acceptance
Notification. You will be notified by the Editor of the journal of the acceptance of your article and invited to supply an electronic version of the accepted text, if this is not already available.
Copyright transfer. You will be asked to transfer the copyright of the article to the Publisher. This transfer will ensure the widest possible dissemination of information.
Proofs. The corresponding author receives proofs, which should be corrected and returned to the publisher within three days of receipt. Please note that typesetting costs of extensive author's corrections in proofs, other than those of printer's errors, will be charged to the author.

Electronic manuscripts
The Publisher welcomes the receipt of an electronic version of your accepted manuscript (preferably encoded in LaTeX). If you have not already supplied the final, revised version of your article (on diskette) to the Journal Editor, you are requested herewith to send a file with the text of the accepted manuscript directly to the Publisher by e-mail or on diskette (allowed formats 3.5" or 5.25" MS-DOS, or 3.5" Macintosh) to the address given below. Please note that no deviations from the version accepted by the Editor of the journal are permissible without the prior and explicit approval by the Editor. Such changes should be clearly indicated on an accompanying printout of the file.

Author benefits
No page charges. Publishing in Mechanics of Materials is free.
Free offprints. The corresponding author will receive 50 offprints free of charge. An offprint order form will be supplied by the Publisher for ordering any additional paid offprints.
Discount. Contributors to Elsevier Science journals are entitled to a 30% discount on all Elsevier Science books.

Further information (after acceptance)

Elsevier Science B.V., Mechanics of Materials
Desk Editorial Department
P.O. Box 103, 1000 AC Amsterdam
The Netherlands
Tel.: + 31 20 4852745
Fax: + 31 20 4852431
E-mail: NHPNUCLEAR@ELSEVIER.NL